Original Article

JCBFM

Journal of Cerebral Blood Flow & Metabolism
2017, Vol. 37(8) 2768–2779

DOI: 10.1177/0271678X16674737
journals.sagepub.com/home/jcbfm
SAGE

Magnetic resonance imaging of local and remote vascular remodelling after experimental stroke

Pavel Yanev[1], Peter R Seevinck[1], Umesh S Rudrapatna[1], Mark JRJ Bouts[1], Annette van der Toorn[1], Karen Gertz[2,3], Golo Kronenberg[2,4], Matthias Endres[2,3,4,5,6], Geralda A van Tilborg[1] and Rick M Dijkhuizen[1]

Abstract

The pattern of vascular remodelling in relation to recovery after stroke remains largely unclear. We used steady-state contrast-enhanced magnetic resonance imaging to assess the development of cerebral blood volume and microvascular density in perilesional and exofocal areas from (sub)acutely to chronically after transient stroke in rats. Microvascular density was verified histologically after infusion with Evans Blue dye. At day 1, microvascular cerebral blood volume and microvascular density were reduced in and around the ischemic lesion (intralesional borderzone: microvascular cerebral blood volume = 72 ± 8%; microvascular density = 76 ± 8%) ($P < 0.05$), while total cerebral blood volume remained relatively unchanged. Perilesional microvascular cerebral blood volume and microvascular density subsequently normalized (day 7) and remained relatively stable (day 70). In remote ipsilateral areas in the thalamus and substantia nigra – not part of the ischemic lesion – microvascular density gradually increased between days 1 and 70 (thalamic ventral posterior nucleus: microvascular density = 119 ± 9%; substantia nigra: microvascular density = 122 ± 8% ($P < 0.05$)), which was confirmed histologically. Our data indicate that initial microvascular collapse, with maintained collateral flow in larger vessels, is followed by dynamic revascularization in perilesional tissue. Furthermore, progressive neovascularization in non-ischemic connected areas may offset secondary neuronal degeneration and/or contribute to non-neuronal tissue remodelling. The complex spatiotemporal pattern of vascular remodelling, involving regions outside the lesion territory, may be a critical endogenous process to promote post-stroke brain reorganization.

Keywords

Angiogenesis, magnetic resonance imaging, stroke recovery, substantia nigra, thalamus

Received 25 June 2016; Revised 1 September 2016; Accepted 8 September 2016

Introduction

Despite considerable advances in understanding of pathophysiological mechanisms after stroke, acute clinical treatment options remain limited, underscoring the need for discovering new effective targets and strategies to improve post-stroke therapy. Beside focal tissue injury in the ischemic lesion, secondary degeneration and remodelling of neuronal and vascular structures may occur in and around the lesion, as well as at remote connected sites.[1] Multiple gradual endogenous mechanisms contribute to tissue restoration, particularly in the lesion borderzone and exofocal areas, where intact tissue is functionally compromised but

[1]Biomedical MR Imaging and Spectroscopy Group, University Medical Center Utrecht, Utrecht, The Netherlands
[2]Department of Neurology, Charité – Universitaetsmedizin Berlin, Berlin, Germany
[3]Center for Stroke Research Berlin, Charité – Universitaetsmedizin Berlin, Berlin, Germany
[4]German Center for Cardiovascular Research (DZHK), Universitaetsmedizin Berlin, Berlin, Germany
[5]German Center for Neurodegenerative Diseases (DZNE), Universitaetsmedizin Berlin, Berlin, Germany
[6]Berlin Institute of Health (BIH), Berlin, Germany

Corresponding author:
Rick M Dijkhuizen, Center for Image Sciences, University Medical Center Utrecht, Heidelberglaan 100, 3584 CX Utrecht, The Netherlands.
Email: r.m.dijkhuizen@umcutrecht.nl

capable of recovering through plasticity of neuronal networks.[2] Vascular modifications, such as angiogenesis, may be critical for neuroplasticity by supporting neurogenesis and synaptogenesis.[3–5] Angiogenesis and increased microvascular density (MVD) have been identified in perilesional regions of stroke patients.[6–8] Multiple studies in rodent stroke models have shown that neovascularization in lesion borderzones contributes to restoration of perfusion and recovery of tissue, which may be therapeutically enhanced.[5,9–16]

In addition to perilesional alterations, secondary tissue changes, including selective neuronal loss, gliosis and microglial activation, occur in remote non-ischemic areas that are connected to the primary lesion.[17–19] For example, magnetic resonance imaging (MRI) studies in patients with a middle cerebral artery (MCA) territory infarct in cortical tissue have demonstrated progressive degeneration of the ipsilateral thalamus, which is located outside the ischemic area.[20–23] In animal MCA occlusion (MCAO) models, these changes, presumably caused by retrograde degeneration of thalamocortical fibres, are mostly localized within the ventral posterior nucleus (VPN) of the thalamus.[24,25] In patients and animals with ischemic damage in the striatum, delayed tissue injury has also been observed in the substantia nigra, which may be explained by retrograde, anterograde or transsynaptic degeneration through striatonigral and nigrostriatal pathways.[26–29]

Most studies on post-stroke secondary changes in the thalamus and substantia nigra have described parenchymal pathology. However, signs of tissue plasticity have also been reported. Ling et al.[30] found newly formed neuronal cells and blood vessels in the non-ischemic ipsilateral VPN with secondary injury after cortical infarction in rats. Furthermore, Hayward et al.[31] identified increased vascular density in the thalamus that was accompanied by significant hyperperfusion chronically after transient MCAO in rats.

Changes in vascularity and haemodynamics after stroke may contribute to pathophysiology as well as plasticity. In vivo elucidation of the spatiotemporal profile of these changes, ideally assessed with imaging techniques,[32] may provide important insights into the nature of cerebrovascular remodelling and its possible role in tissue outcome after stroke. Therefore, the goal of this study was to characterize the pattern of vascular reorganization in and around the ischemic lesion and in secondarily affected areas (i.e. the thalamus and substantia nigra) from subacute to chronic time-points after transient focal cerebral ischemia. To this aim, we applied steady-state contrast-enhanced (ssCE-)MRI with a long-circulating blood pool agent to quantify various properties of the vascular network, including total and microvascular cerebral blood volume (CBV) and MVD,[33] in relation to tissue damage, from acute to chronic phases after experimental stroke in rats.

Materials and methods

All animal procedures were approved by the Ethical Committee on Animal Experiments of the University Medical Center Utrecht and Utrecht University, and conducted in accordance with the guidelines set by the European Community Council Directives 86/609/EEC. Experiments are reported in compliance with the ARRIVE guidelines (Animal Research: Reporting in Vivo Experiments).

Animal model

Focal cerebral ischemia was induced by 60-min MCAO with an intraluminal filament in rats as described previously.[34]

Adult male Wistar rats (300–330 g) (Harlan, Horst, The Netherlands) were endotracheally intubated and mechanically ventilated with a mixture of air/oxygen (7/1) and 2% isoflurane. The right common carotid artery was exposed through a cervical incision and carefully separated from the adjacent sympathetic nerves. The right common carotid artery and the internal carotid artery were clamped with microvascular clips. The external carotid artery was ligated distally with a nylon suture and electrocoagulated. A 4–0 surgical nylon suture coated with silicon (Doccol, Redlands, CA, USA) was advanced into the internal carotid artery until resistance was felt. The filament was held in place for 60 min by tightening a suture around the internal carotid artery.

During animal surgery, core temperature was maintained at 37.5°C by a temperature-controlled heating pad. Preoperatively, animals received a subcutaneous injection of 0.05 mg/kg buprenorphin (Reckitt & Coman, Kingston-Upton-Hill, UK) for pain relief. To compensate for water and mineral loss, 2.5 mL Ringer's lactate solution (Baxter, Utrecht, The Netherlands) was administered subcutaneously immediately before and after operation, and subsequently 5 mL was given once daily for the first 3–5 days post-surgery. All rats were given ad libitum access to food and water, and were pair-housed in a temperature-controlled environment (20 ± 1°C) with lights on from 07:00 to 19:00 h. Body weight and overall animal well-being were monitored on a daily basis. If weight loss continued for more than 5 days, or if weight decreased below 80% of original body weight, the animal was euthanized to avoid further suffering.

Sixteen rats were included in this study. Rats were scanned at 1 (n = 5), 7 (n = 5), 21 (n = 9) and 70 days (n = 9) after stroke, of which 4 animals were scanned

serially at all time-points, while 12 animals were scanned at single time-points.

MRI

MRI measurements were performed using a 4.7 T/40 cm horizontal bore MR system (Agilent Technologies Inc., Palo Alto, CA, USA). A custom-built (2.5-cm diameter) surface coil was used for signal reception, while a Helmholtz volume coil was used for radio-frequency transmission.

Rats were secured in a MR-compatible cradle using ear bars and a bite bar, and anaesthesia was maintained in the same manner as described for the MCAO procedure. Blood oxygenation, expired CO_2 and heart rate were continuously measured throughout imaging, and kept within physiological range. Core temperature was maintained at 37.5°C.

For ssCE-MRI, we used a multi-slice multi-spin-echo (SE) (repetition time (TR)/first echo time (TE_1)/echo time interval (ΔTE) = 3500/13/13 ms; 12 echoes), and a multi-slice multi-gradient echo (GE) ($TR/TE_1/\Delta TE = 1800/4/4$ ms; 25 echoes) sequence with 19 slices of 1-mm slice thickness, field-of-view (FOV) of $30 \times 30\,mm^2$, data matrix size of 256×128 (frequency encoding × phase encoding) and two averages. SE and GE images were acquired before and after intravenous bolus injection of long circulating ultrasmall particles of iron oxide (USPIO), with a hydrodynamic diameter of 25–30 nm (P904, Guerbet Research, Aulnay-sous-Bois, France). USPIO was introduced via a catheter in the tail vein to achieve a total dose of 300 μmol Fe/kg (~16.8 mg Fe/kg). Post-contrast SE and GE acquisition was started 5 min after contrast agent injection to reach a steady state. Total scan duration was approximately 135 min.

Image processing and analysis

All parametric maps were obtained on a voxel-by-voxel level, using MATLAB (MathWorks, Natick, MA, USA). Transverse relaxation rate changes ΔR_2 and ΔR_2^*, were calculated as $\Delta R_2 = 1/T_{2\ post} - 1/T_{2\ pre}$ and $\Delta R_2^* = 1/T_2^*{}_{post} - 1/T_2^*{}_{pre}$, where $T_{2\ pre}$, $T_{2\ post}$ and $T_2^*{}_{pre}$, $T_2^*{}_{post}$ are the pre- and post-contrast T_2 and T_2^* values obtained from the SE and GE acquisitions, respectively. ΔR_2 is a measure of primarily microvascular blood volume (e.g. in capillaries and venules), whereas ΔR_2^* reflects total blood volume, including large vessels.[35,36] The parameter Q, an estimate of MVD, was calculated as $\Delta R_2/(\Delta R_2^*)^{2/3}$.[37,38] Voxels with negative ΔR_2 and ΔR_2^* values were assigned a Q value equal to zero to eliminate non-biological values.

T_2 maps, calculated from the pre-contrast SE acquisition, were spatially aligned to a reference image template created from six control rat brains, using non-rigid coregistration.[39] Brain parenchyma was automatically segmented from surrounding tissue using a brain extraction tool.[40] T_2 maps from all animals were averaged, and the mean T_2 value and its standard deviation (SD) in normal grey matter were calculated. For each individual animal, voxels with T_2 values above the mean plus 4.5 SD were identified as cerebrospinal fluid and excluded from further analyses.

A contralateral region-of-interest (ROI) encompassing cortical and subcortical grey matter tissue in the unaffected hemisphere was defined based on the coregistered image template guided by an anatomical atlas[41] (Figure 1(a)). The lesion volume was automatically determined on pre-contrast T_2 maps, defined as tissue with T_2 values above the mean plus 2SD of contralateral tissue values. The resulting volume was median-filtered, binarized and eroded radially by 9 voxels using a 2D kernel, which provided a *lesion core* ROI (Figure 1(a)). An *intralesional borderzone* ROI was created by subtracting the lesion core volume from the total lesion volume (Figure 1(a)). Dilating the total lesion volume by 9 voxels (2D kernel), and subtracting the resultant volume with the total lesion volume provided an *extralesional borderzone* ROI (Figure 1(a)). In addition, the ipsilateral *thalamic VPN* and the *substantia nigra* were manually delineated on pre-contrast T_2 maps (Figure 1(b)), guided by a superimposed anatomical atlas[41] using FMRIB Software Library (FSL, http://www.fmrib.ox.ac.uk/fsl). Homologous ROIs in the contralateral VPN and substantia nigra were automatically generated, with corrections for midline shift and tissue shrinkage. The processing algorithm was compiled in MATLAB (MathWorks, Natick, MA, USA). In each ipsi- and contralateral ROI we calculated the mean value of $T_{2\ pre}$, $T_2^*{}_{pre}$, ΔR_2, ΔR_2^* and Q.

Evans Blue perfusion of vessels

After the final MRI scan at day 70, in 8 rats vascular density was assessed as described by Gertz et al. in detail previously.[16,42] Briefly, anaesthesia was maintained as during MRI. Endovascular dye Evans Blue (Sigma-Aldrich; 1 mL of 2% solution in saline) was infused through the same tail vain catheter as used for contrast agent injection. 5 min after infusion, animals were decapitated and brains were snap-frozen. Brain tissue was cut in 10 μm coronal cryosections. Digitized fluorescence microscopy images were acquired with a cooled-CCD camera (CoolSNAP EZ, Photometrics, Tucson, AZ, USA), attached to a fluorescence microscope. Microscopic resolution images of whole brain sections were acquired by joining together single images using tiled-field mapping software

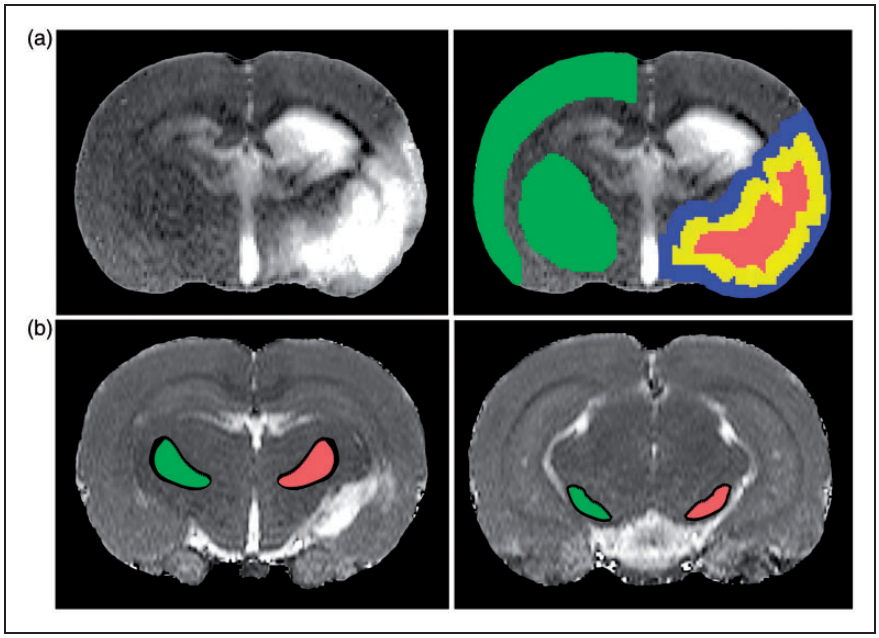

Figure 1. T_2 maps of coronal brain slices depicting the regions-of-interest (ROIs). (a) Lesioned tissue was indentified by elevated T_2 values (left image). Total lesion volume (red and yellow ROIs combined) was calculated from ipsilateral tissue voxels with T_2 values 2SD above the mean of values in contralateral grey matter (superimposed on normalized T_2 maps) (right image). Subsequent automated image processing (i.e. erosion and dilation) generated three ROIs: lesion core (red), intralesional borderzone (yellow) and extralesional borderzone (blue). A contralateral ROI (green) encompassing cortical and subcortical tissue was manually selected. (b) Ipsi- (red) and contralateral ROIs (green) of the VPN (left image) and SN (right image) were manually outlined on posterior slices.

(MCID 7.0 Elite; Interfocus Imaging, Linton, UK). The technique of density slicing was used for ROI specification including the setting of target acceptance criteria.[16,42,43] Microvessel counts were performed by G.K. who was blinded for the MRI findings.

Statistical analysis

An ANOVA was performed across time points, and differences between corresponding ROIs in the ipsi- and contralateral hemispheres were evaluated with a paired t-test. Values are shown as mean $\pm$ SD. $P < 0.05$ was considered significant.

Results

Transient unilateral MCAO resulted in an ipsilateral lesion, characterized by tissue with clearly elevated T_2 values, which included the striatum and cortex, without involvement of the thalamus and substantia nigra (Figure 1).

Figure 2 shows representative maps of the T_2 (tissue integrity), ΔR_2 (microvascular CBV), ΔR_2* (total CBV) and Q (MVD) in brain slices encompassing the primary lesion (Figure 2(a)), the thalamus (Figure 2(b)) and the substantia nigra (Figure 2(c)) of a single rat at 1, 7, 21 and 70 days after MCAO. ΔR_2* and ΔR_2 maps revealed substantial temporal alterations in- and outside the lesion territory, as well as in remote ipsilateral subcortical areas, i.e. the thalamus and substantia nigra. No significant temporal changes in T_2, T_2*, ΔR_2*, ΔR_2 or Q were observed in the contralateral ROIs (see also Figure 3).

Spatiotemporal alterations in the primary lesion area

During the course of 70 days after stroke, T_2 changes in the primary lesion reflected oedema formation (day 1), pseudo-normalization in grey matter accompanied by white matter oedema (day 7) and ultimately liquefaction and tissue shrinkage (days 21 and 70) (Figure 2(a)). Lesion volumes were $165 \pm 71\,mm^3$ at day 1, $164 \pm 100\,mm^3$ at day 7, $115 \pm 96\,mm^3$ at day 21 and $146 \pm 84\,mm^3$ at day 70. Figure 3(a), which displays the quantitative results from ROI analysis, shows that T_2 was significantly prolonged at day 1 in all lesional ROIs, particularly in the lesion core and intralesional borderzone, where values continued to further increase until day 70. T_2* was also prolonged in the lesion core, which progressed over time, whereas T_2* was shortened in the extralesional borderzone at post-stroke days 7 to 70.

At day 1 after stroke, ΔR_2 (microvascular CBV) and Q (MVD) were significantly decreased in the entire

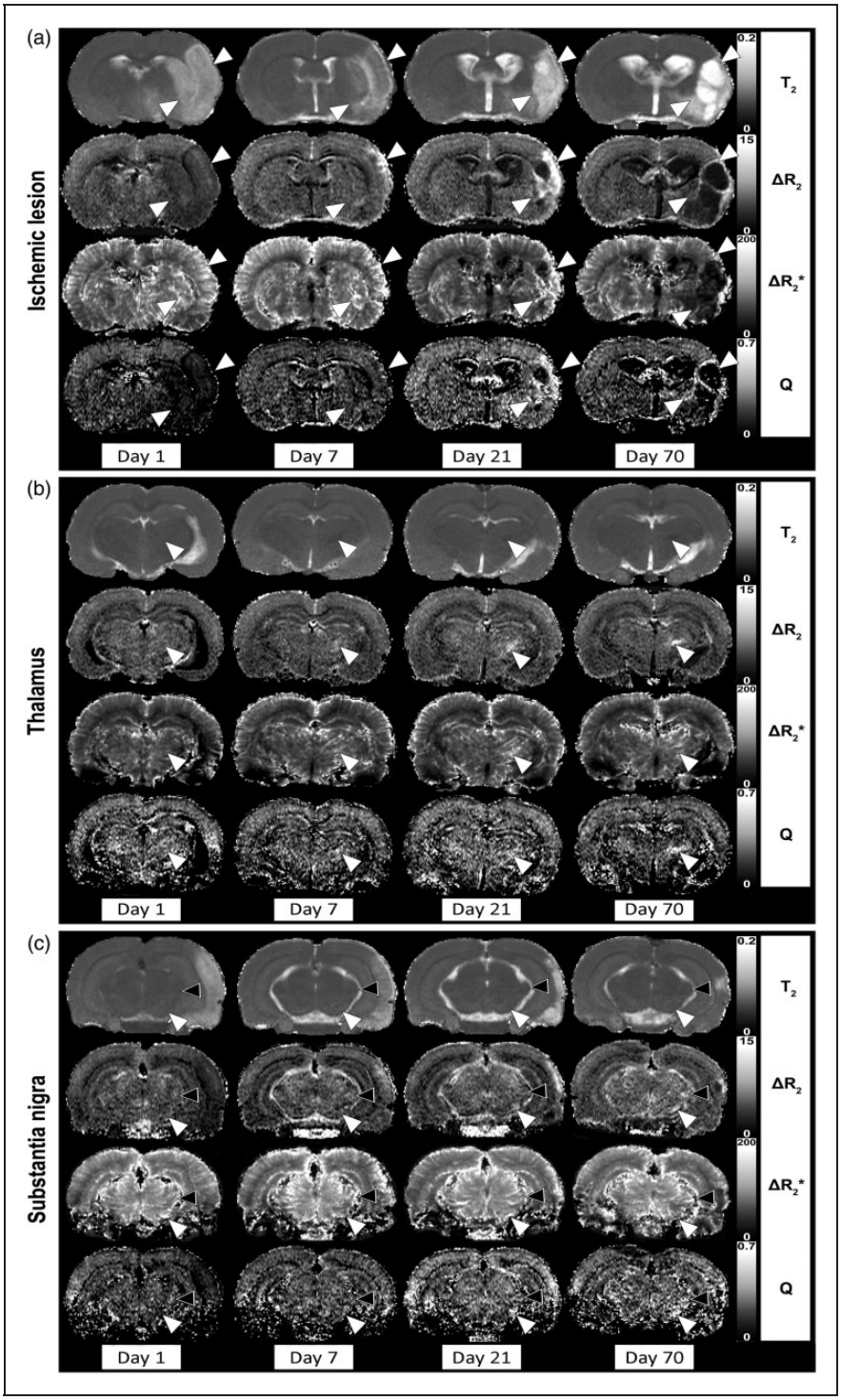

Figure 2. Quantitative maps of pre-contrast T_2, ΔR_2 (microvascular CBV), ΔR_2^* (total CBV) and Q (MVD) in rat brain at different time-points after 60-min unilateral MCAO. Maps of coronal rat brain slices are shown at the level of the primary lesion site (cortical and striatal borderzones depicted by white arrowheads) (a), thalamus (VPN depicted by white arrowheads) (b) and substantia nigra (white arrowheads) and medial geniculate nucleus (black arrowheads) (c).

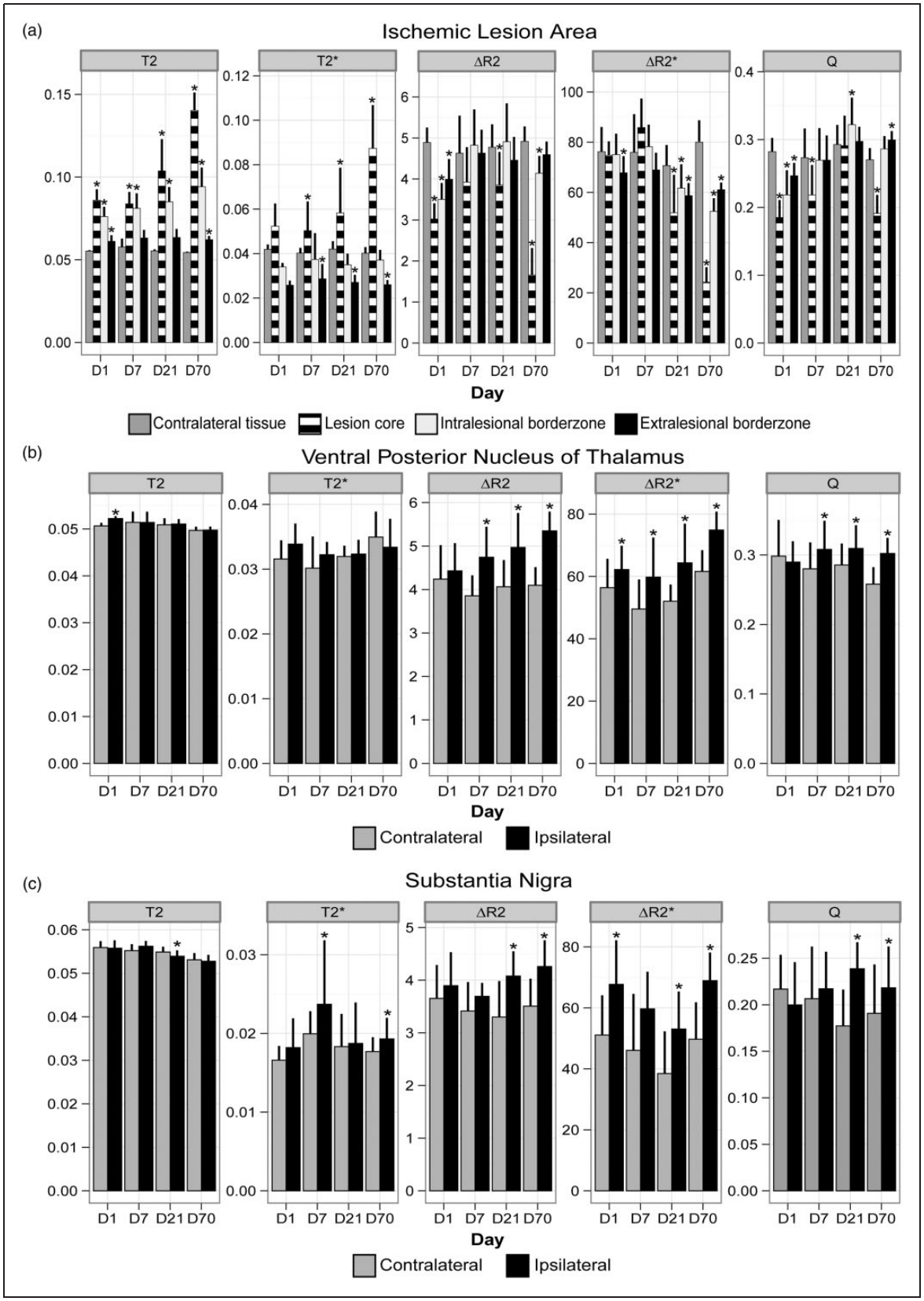

Figure 3. Pre-contrast T_2 (s), pre-contrast T_2* (s), ΔR_2 (s^{-1}), ΔR_2* (s^{-1}) and Q ($s^{-1/3}$) (mean $\pm$ SD) in lesional ROIs (a), VPN (b) and substantia nigra (c) at different post-stroke time-points. *$P < 0.05$ versus contralateral ROI.

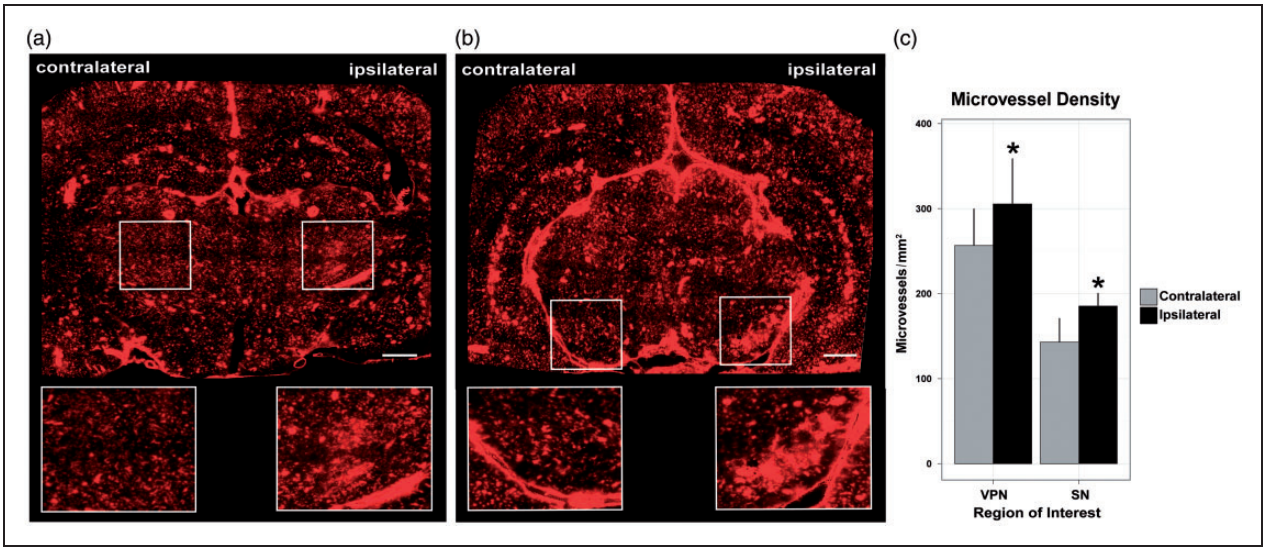

Figure 4. Respective micrographs of coronal sections showing Evans Blue-perfused microvessels at the level of the thalamic VPN (a), and substantia nigra (b) of a rat at 70 days after 60-min unilateral MCAO. ROIs selected for vessel counting are depicted by the boxes. Scale bar: (a,b) = 1000 μm. (c) Density of Evans Blue-filled microvessels (n/mm^2) in ipsi- and contralateral ROIs. *$P < 0.05$ versus contralateral.

lesion area. However, ΔR_2* (total CBV) was relatively unchanged compared with corresponding areas in the contralateral hemisphere, except for the extralesional borderzone. At day 7, ΔR_2 was largely restored in intra- and extralesional areas. Normalization of Q was also apparent around the lesion territory, except for in the core where it remained low. ΔR_2* was relatively unaffected at this time point. After 21 days, increased ΔR_2 and Q were observed in perilesional regions. ΔR_2* values in perilesional tissue were more variable and included elevated as well as lowered values. On average, ΔR_2* was reduced in all lesional ROIs. At day 70, ΔR_2*, ΔR_2 and Q were significantly reduced in the lesion core. ΔR_2*, ΔR_2 and Q in lesion borderzones remained relatively higher, although to a lesser extent as compared with day 21 (e.g. intralesional ΔR_2 was significantly lower at this stage).

To confirm the observed temporal patterns, we separately analysed the four rats that were scanned serially at all time points. Results are shown in Supplementary Fig. 1, which clearly demonstrate the same trends for all parameters.

Spatiotemporal alterations in remote regions: Thalamus and substantia nigra

Beside the clear alterations in and around the primary lesion site, mild to moderate temporal changes on the parameteric MRI maps were detected in remote subcortical regions, including the thalamus (Figure 2(b)) and substantia nigra (Figure 2(c)). These changes were most evident in the VPN. Occasionally, similar effects were observed in the ipsilateral medial geniculate nucleus (Figure 2(c), black arrowheads), particularly in animals with substantial damage in the auditory cortex. At post-stroke day 1, a minor but significant prolongation of T_2 was detected in the ipsilateral VPN, which slowly declined thereafter (Figure 3(b)). To lesser extent, this was also observed in the ipsilateral substantia nigra (Figure 3(c)), where we also measured significant T_2* prolongation at days 7 and 70.

Vascular parameters revealed substantial changes in the ipsilateral VPN and substantia nigra over time (Figure 3(b) and (c)). ΔR_2* was significantly increased in the VPN and substantia nigra from day 1 to 70, except for day 7 in the substantia nigra. Significant elevations of ΔR_2 and Q were evident from day 7 onwards in the VPN, and from day 21 onwards in the substantia nigra.

Separate analysis of the serially measured cohort corroborated the observed temporal trends (Supplementary Fig. 1).

Evaluation of vascularity in the VPN and substantia nigra

Fluorescence microscopy images of brain sections from Evans Blue-perfused animals after the last MRI timepoint, revealed increased vascularity in the ipsilateral VPN (Figure 4(a)) and substantia nigra (Figure 4(b)). Results from vessel counting showed that the density of microvessels was significantly increased in the ipsilateral VPN ($116 \pm 5\%$) and substantia nigra ($119 \pm 10\%$), as compared with the contralateral homologous area ($P < 0.05$) (Figure 4(c)).

Discussion

We employed ssCE-MRI to quantitatively assess the effects of transient focal cerebral ischemia on the perfused vasculature during long-term recovery from stroke. Using a 60-min MCAO model in rats, we identified temporally characteristic changes in total CBV (ΔR_2*), microvascular CBV and MVD (Q) in different ipsilateral areas. These vascular alterations were not restricted to the lesion site and its borderzones, however, but also included remote regions, i.e. the ipsilateral thalamus and the substantia nigra. Our data demonstrate a gradual increase in (total and microvascular) CBV and MVD, which persisted for at least 3 months after stroke and was confirmed histologically.

Vascular remodelling in and around the ischemic lesion

One day after transient ischemia, the lesion area (characterized by prolonged tissue T_2 due to vasogenic oedema[44]) displayed decreased microvascular CBV and MVD, while total CBV was largely unchanged. Increased pressure due to oedema may cause microvessels to collapse, leading to the observed reduction in microvascular CBV and MVD. Higher total CBV could occur due to early vasodilation or arteriogenesis of collateral vessels,[9] which compensate for the lower cerebral blood flow (CBF) in the ischemic territory. Correspondingly, improved collateral flow by an increase in total CBV, as opposed to unchanged or lowered microvascular CBV, has been observed in the rat cortex early after ischemia–reperfusion in an earlier ssCE-MRI study.[45]

Extensive initial oedema in grey matter, as depicted on T_2 maps, largely subsided by post-stroke day 7, consistent with other reports on transient T_2 normalization in lesioned tissue after stroke.[46–48] This was accompanied by normalization of microvascular CBV and MVD in the lesion border areas. Levels of these parameters remained significantly lowered in the lesion core, except for a transient elevation of the MVD in the core region at day 21, which may be (partly) explained by methodological issues, as described below. Earlier serial ssCE-MRI studies in rats reported a gradual increase of microvascular CBV and/or MVD, following initial reductions in the ischemic lesion territory.[40,45,49,50] Still, the pattern of vascular changes strongly depends on the extent to which tissue is damaged after stroke. While the ischemic core is predominantly necrotic, particularly at chronic stages, the surrounding area is a mixture of necrotic, apoptotic, rearranging and normal parenchyma.[48,51]

Precise lesion segmentation on MR images, however, is difficult as there are no uniform signal differences between the lesion core, the lesion borderzones and unaffected tissue. Therefore, we applied an automated region growing and shrinking approach to differentiate between the lesion core, and extra- and intralesional borderzones, respectively. In the intralesional borderzone, we observed a dynamic temporal development of post-ischemic CBV and MVD changes accompanied by continuously elevated tissue T_2. This reflects an active and heterogeneous tissue experiencing the formation and subsequent regression of new undeveloped (leaky) vessels, in line with findings in another study.[47] The extralesional borderzone, on the other hand, displayed a more gradual and steady increase in microvascular CBV and MVD, which suggests angiogenesis leading to a stable vascular network. Moreover, this area exhibited a significantly lower T_2*, which has been associated with newly developed mature vasculature.[52] However, other factors, such as enhanced macrophage activity, may also explain T_2* shortening in perilesional tissue.[53]

Neovascularization in post-stroke brain may indicate a higher demand for vascular support in areas undergoing active neural tissue reorganization. Correspondingly, earlier studies have shown a close association of the dynamics of angiogenesis with neurogenesis (evidenced from specific migration of neuroblasts through areas that exhibited vascular remodelling and increased vessel density[3,4]), as well as dendritic plasticity (evidenced from paralleled orientation of remodelling dendritic and vascular segments[54]) in perilesional areas. Furthermore, therapeutic interventions, e.g. cell-based therapies, that concurrently enhance vascular and neuronal remodelling, have shown to be effective in improving functional recovery in preclinical stroke models.[5] On the other hand, neovascularization has also been shown to occur in concomitance with astrogliosis,[55] which suggests that post-stroke vascular remodelling may also contribute to formation of non-neuronal scar tissue. Future studies should provide further insights in the mechanisms and role of the formation of new vasculature after stroke.

Stroke-induced vascular remodelling in remote areas

Beside the intra- and perilesional vascular alterations, we detected significant changes in remote brain regions that were not part of the primary ischemic stroke lesion. Particularly, the ipsilateral VPN of the thalamus and the substantia nigra had chronically elevated CBV and MVD levels. Microscopic examination of histological brain sections revealed a greater number of microvessels in these regions.

Secondary exofocal neuronal damage in regions remote from a primary ischemic lesion, due to retrograde, anterograde or transsynaptic degeneration of connected tissue, is a well-known phenomenon.[18] Histopathological studies in rodent stroke models

have shown neuronal loss, axonal injury and glial activation in the non-ischemic thalamus and substantia nigra following cortical or striatal infarction, respectively.[19,24,25,34,56–61] The transient T_2 and T_2* changes that we detected in the VPN and substantia nigra could reflect ongoing neurodegeneration and neuroinflammation, in line with previous observations from MRI in stroke patients[23,28] and animal models.[34,56–58] Yet, the occurrence of vascular remodelling in remote regions anatomically connected to the primary lesion site is a relatively unknown phenomenon.

Ling et al.[30] found that post-stroke secondary degeneration in the thalamus may be accompanied by angiogenesis and neurogenesis. In addition to neuronal loss and microglial activation in the ipsilateral VPN at days 7 and 14 after cortical infarction in rats, immunohistochemical analysis revealed proliferating neural and endothelial cells as well as increased vessel density in the VPN. In a perfusion MRI study by Hayward et al.,[31] it was shown that CBF progressively increases in the ipsilateral thalamus, while cortical CBF remained lowered, between 2 days and 3 months after transient MCAO in rats. Furthermore, these authors showed that the number of branching vessel points after 3 months was significantly higher in the ipsilateral thalamus as compared with contralateral. Our present study provides further evidence of progressive microvascularization in the thalamus, specifically in the VPN, after ischemic damage to the sensorimotor cortex and striatum. The rise in total CBV may suggest that recruitment or reinforcement of larger vessels (arteriogenesis) may also be part of the vascular remodelling. Importantly, we detected similar changes in the ipsilateral substantia nigra (and in the medial geniculate nucleus in animals with ischemic injury to the auditory cortex), which indicates that post-stroke angiogenesis and/or arteriogenesis may be a common process in remote connected brain regions with secondary tissue degeneration.

Advantages and limitations of ssCE-MRI for vascular imaging

Using MRI to assess cerebrovascular remodelling offers the advantage of in vivo, serial and whole-brain monitoring with simultaneous measurement of brain tissue injury. Because ssCE-MRI is based on signal from a circulating intravascular contrast agent, only perfused (functional) vessels are detected. This is in contrast to histological assessment by post mortem staining of vascular structures, which may include non-functional vessels. Furthermore, different traits of the cerebrovasculature, such as microvascular and total CBV, as well as MVD, can be characterized. However, there are also limitations to the ssCE-MRI-based approach. In the current study, we used the parameter Q as a measure of MVD,[37,38] but more accurate quantification of MVD values may be feasible with additional input of the local tissue diffusion coefficient.[33] Since diffusion depends on tissue microstructure, values can vary considerably in different tissue types and under pathological conditions. In a recent article by Boehm-Sturm et al.,[49] it was shown that MVD measures may be overestimated when diffusion is high, such as in a cystic lesion chronically after stroke. This could explain the high ΔR_2 and Q values that we observed in some regions inside the lesion core at chronic stages. Furthermore, Boehm-Sturm et al. reported that ΔR_2 calculations may vary between single- and multi-echo MRI protocols. Future ssCE-MRI studies should further evaluate how different MRI acquisition schemes affect the quantification of different vascular measures to determine the most optimal imaging protocol for assessing vascularity in tissues.

To verify the reliability of our ssCE-MRI data, we directly compared MRI-based MVD findings with vessel counts. Intravenous injections of Evans Blue dye after the final MRI session on post-stroke day 70, allowed the specific detection of perfused vessels similar to ssCE-MRI. We limited vessel quantification to the thalamus and substantia nigra, which were structurally intact after tissue processing. The greater number of microvessels in the ipsilateral thalamus and substantia nigra is in agreement with our ssCE-MRI-based MVD measurements, corroborating Q as a measure of the density of perfused microvasculature.

Conclusions

While early recovery from acute stroke is associated with oedema resolution and re-establishment of circulation in perilesional tissue, ongoing structural and functional reorganization in extended ipsilateral and contralateral neuronal networks is believed to contribute to long-term restoration of functions.[62–66] Our data indicate that large-scale vascular remodelling plays a dynamic, long-term role in the reorganizational processes in the brain after stroke. Vascular reorganization follows a complex spatiotemporal pattern in and around the lesion, as well as remote associated areas, namely the substantia nigra and thalamus. At early time points, vasodilation and arteriogenesis of larger vessels may temporarily compensate for microvascular compression in the ischemic territory. The subsequent transient increase in microvascular perfusion in perilesional areas may reflect the formation of new vessels, which could locally contribute to neuronal survival, clearance of debris[67] and scar formation. Furthermore, a gradual increase in microvessel densities in the extralesional borderzone and remote areas

with secondary tissue degeneration suggests that angiogenesis could support reorganization and restoration of neural networks. Since vascular remodelling after stroke may play a critical role in endogenous neuroprotection and neurorepair, it should be considered as a factor in advancing therapeutic strategies to improve neurological outcome in stroke patients, which may be effectively monitored with ssCE-MRI.

Funding

The author(s) disclosed receipt of the following financial support for the research, authorship, and/or publication of this article: The European Union's Seventh Framework Programme (FP7/2007-2013) under grant agreements no. 201024 and no. 202213 (European Stroke Network to R.M.D. and M.E.), the Netherlands Organization for Scientific Research (NWO) (VIDI 917.76.347; VICI 016.130.662 to R.M.D.), the Deutsche Forschungsgemeinschaft (SFB TRR43 and Exc257 to M.E.; KR 2956/4-1 to G.K.; GE 2576/2-1 to K.G.), the Bundesministerium für Bildung und Forschung (CSB to M.E. K.G. and G.K.), the German Center for Neurodegenerative Diseases (DZNE to M.E.), and the German Center for Cardiovascular Research (DZHK to M.E.); Transatlantic Networks of Excellence Program from the Foundation Leducq (to M.E.).

Acknowledgements

The authors thank Dr. Ann Stowe for the valuable contributions regarding the improvement of quality and coherence of the manuscript.

Declaration of conflicting interests

The author(s) declared no potential conflicts of interest with respect to the research, authorship, and/or publication of this article.

Authors' contributions

PY and RMD designed the studies, interpreted data and drafted the manuscript; PY, RMD, PRS, USR, KG, GK, ME and GAT executed experiments and/or analysed data; USR, MJB and AT provided analytical software support. All authors revised and approved the final submission.

Supplementary material

Supplementary material for this paper can be found at http://jcbfm.sagepub.com/content/by/supplemental-data

References

1. Stowe AM, Plautz EJ, Eisner-Janowicz I, et al. VEGF protein associates to neurons in remote regions following cortical infarct. *J Cereb Blood Flow Metab* 2007; 27: 76–85.
2. Dijkhuizen RM. Imaging neuronal loss and recovery in compromised but viable brain tissue. *Brain* 2013; 136: 1689–1691.
3. Ohab JJ, Fleming S, Blesch A, et al. A neurovascular niche for neurogenesis after stroke. *J Neurosci* 2006; 26: 13007–13016.
4. Thored P, Wood J, Arvidsson A, et al. Long-term neuroblast migration along blood vessels in an area with transient angiogenesis and increased vascularization after stroke. *Stroke* 2007; 38: 3032–3039.
5. Xiong Y, Mahmood A and Chopp M. Angiogenesis, neurogenesis and brain recovery of function following injury. *Curr Opin Investig Drugs* 2010; 11: 298–308.
6. Krupinski J, Kaluza J, Kumar P, et al. Role of angiogenesis in patients with cerebral ischemic stroke. *Stroke* 1994; 25: 1794–1798.
7. Slevin M, Krupinski J, Slowik A, et al. Serial measurement of vascular endothelial growth factor and transforming growth factor-beta1 in serum of patients with acute ischemic stroke. *Stroke* 2000; 31: 1863–1870.
8. Szpak GM, Lechowicz W, Lewandowska E, et al. Border zone neovascularization in cerebral ischemic infarct. *Folia Neuropathol* 1999; 37: 264–268.
9. Liu J, Wang Y, Akamatsu Y, et al. Vascular remodeling after ischemic stroke: mechanisms and therapeutic potentials. *Prog Neurobiol* 2014; 115: 138–156.
10. Hayashi T, Deguchi K, Nagotani S, et al. Cerebral ischemia and angiogenesis. *Curr Neurovasc Res* 2006; 3: 119–129.
11. Slevin M, Kumar P, Gaffney J, et al. Can angiogenesis be exploited to improve stroke outcome? Mechanisms and therapeutic potential. *Clin Sci* 2006; 111: 171–183.
12. Arai K, Jin G, Navaratna D, et al. Brain angiogenesis in developmental and pathological processes: neurovascular injury and angiogenic recovery after stroke. *FEBS J* 2009; 276: 4644–4652.
13. Beck H and Plate KH. Angiogenesis after cerebral ischemia. *Acta Neuropathol* 2009; 117: 481–496.
14. Ergul A, Alhusban A and Fagan SC. Angiogenesis: a harmonized target for recovery after stroke. *Stroke* 2012; 43: 2270–2274.
15. Liman TG and Endres M. New vessels after stroke: postischemic neovascularization and regeneration. *Cerebrovasc Dis* 2012; 33: 492–499.
16. Gertz K, Priller J, Kronenberg G, et al. Physical activity improves long-term stroke outcome via endothelial nitric oxide synthase-dependent augmentation of neovascularization and cerebral blood flow. *Circ Res* 2006; 99: 1132–1140.
17. Baron JC, Yamauchi H, Fujioka M, et al. Selective neuronal loss in ischemic stroke and cerebrovascular disease. *J Cereb Blood Flow Metab* 2014; 34: 2–18.
18. Zhang J, Zhang Y, Xing S, et al. Secondary neurodegeneration in remote regions after focal cerebral infarction: a new target for stroke management? *Stroke* 2012; 43: 1700–1705.
19. Kronenberg G, Balkaya M, Prinz V, et al. Exofocal dopaminergic degeneration as antidepressant target in mouse model of poststroke depression. *Biol Psychiatry* 2012; 72: 273–281.
20. Tamura A, Tahira Y, Nagashima H, et al. Thalamic atrophy following cerebral infarction in the territory of the middle cerebral artery. *Stroke* 1991; 22: 615–618.

21. De Reuck J, Decoo D, Lemahieu I, et al. Ipsilateral thalamic diaschisis after middle cerebral artery infarction. *J Neurol Sci* 1995; 134: 130–135.
22. Nakane M, Tamura A, Sasaki Y, et al. MRI of secondary changes in the thalamus following a cerebral infarct. *Neuroradiology* 2002; 44: 915–920.
23. Ogawa T, Yoshida Y, Okudera T, et al. Secondary thalamic degeneration after cerebral infarction in the middle cerebral artery distribution: evaluation with MR imaging. *Radiology* 1997; 204: 255–262.
24. Iizuka H, Sakatani K and Young W. Neural damage in the rat thalamus after cortical infarcts. *Stroke* 1990; 21: 790–794.
25. Dihne M, Grommes C, Lutzenburg M, et al. Different mechanisms of secondary neuronal damage in thalamic nuclei after focal cerebral ischemia in rats. *Stroke* 2002; 33: 3006–3011.
26. Forno LS. Reaction of the substantia nigra to massive basal ganglia infarction. *Acta Neuropathol* 1983; 62: 96–102.
27. Ogawa T, Okudera T, Inugami A, et al. Degeneration of the ipsilateral substantia nigra after striatal infarction: evaluation with MR imaging. *Radiology* 1997; 204: 847–851.
28. Nakane M, Teraoka A, Asato R, et al. Degeneration of the ipsilateral substantia nigra following cerebral infarction in the striatum. *Stroke* 1992; 23: 328–332.
29. Winter B, Brunecker P, Fiebach JB, et al. Striatal infarction elicits secondary extrafocal MRI changes in ipsilateral substantia nigra. *PLoS One* 2015; 10: e0136483.
30. Ling L, Zeng J, Pei Z, et al. Neurogenesis and angiogenesis within the ipsilateral thalamus with secondary damage after focal cortical infarction in hypertensive rats. *J Cereb Blood Flow Metab* 2009; 29: 1538–1546.
31. Hayward NM, Yanev P, Haapasalo A, et al. Chronic hyperperfusion and angiogenesis follow subacute hypoperfusion in the thalamus of rats with focal cerebral ischemia. *J Cereb Blood Flow Metab* 2011; 31: 1119–1132.
32. Yanev P and Dijkhuizen RM. In vivo imaging of neurovascular remodeling after stroke. *Stroke* 2012; 43: 3436–3441.
33. Seevinck PR, Deddens LH and Dijkhuizen RM. Magnetic resonance imaging of brain angiogenesis after stroke. *Angiogenesis* 2010; 13: 101–111.
34. Longa EZ, Weinstein PR, Carlson S, et al. Reversible middle cerebral artery occlusion without craniectomy in rats. *Stroke* 1989; 20: 84–91.
35. Boxerman JL, Hamberg LM, Rosen BR, et al. MR contrast due to intravascular magnetic susceptibility perturbations. *Magn Reson Med* 1995; 34: 555–566.
36. Kiselev VG, Strecker R, Ziyeh S, et al. Vessel size imaging in humans. *Magn Reson Med* 2005; 53: 553–563.
37. Jensen JH and Chandra R. MR imaging of microvasculature. *Magn Reson Med* 2000; 44: 224–230.
38. Wu EX, Tang HY and Jensen JH. High-resolution MR imaging of mouse brain microvasculature using the relaxation rate shift index Q. *NMR Biomed* 2004; 17: 507–512.
39. Klein S, Staring M, Murphy K, et al. elastix: a toolbox for intensity-based medical image registration. *IEEE Trans Med Imaging* 2010; 29: 196–205.
40. Smith SM. Fast robust automated brain extraction. *Hum Brain Mapp* 2002; 17: 143–155.
41. Paxinos G and Watson C. *The rat brain in stereotaxic coordinates*, 5th ed. San Diego: Elsevier Academic Press, 2005.
42. Gertz K, Kronenberg G, Kalin RE, et al. Essential role of interleukin-6 in post-stroke angiogenesis. *Brain* 2012; 135: 1964–1980.
43. Gobel U, Theilen H and Kuschinsky W. Congruence of total and perfused capillary network in rat brains. *Circ Res* 1990; 66: 271–281.
44. Dijkhuizen RM and Nicolay K. Magnetic resonance imaging in experimental models of brain disorders. *J Cereb Blood Flow Metab* 2003; 23: 1383–1402.
45. Lin CY, Chang C, Cheung WM, et al. Dynamic changes in vascular permeability, cerebral blood volume, vascular density, and size after transient focal cerebral ischemia in rats: evaluation with contrast-enhanced magnetic resonance imaging. *J Cereb Blood Flow Metab* 2008; 28: 1491–1501.
46. Lin SP, Schmidt RE, McKinstry RC, et al. Investigation of mechanisms underlying transient T2 normalization in longitudinal studies of ischemic stroke. *J Magn Reson Imaging* 2002; 15: 130–136.
47. Wagner DC, Deten A, Hartig W, et al. Changes in T2 relaxation time after stroke reflect clearing processes. *Neuroimage* 2012; 61: 780–785.
48. Wegener S, Weber R, Ramos-Cabrer P, et al. Temporal profile of T2-weighted MRI distinguishes between pannecrosis and selective neuronal death after transient focal cerebral ischemia in the rat. *J Cereb Blood Flow Metab* 2006; 26: 38–47.
49. Boehm-Sturm P, Farr TD, Adamczak J, et al. Vascular changes after stroke in the rat: a longitudinal study using optimized magnetic resonance imaging. *Contrast Media Mol Imaging* 2013; 8: 383–392.
50. Moisan A, Favre IM, Rome C, et al. Microvascular plasticity after experimental stroke: a molecular and MRI study. *Cerebrovasc Dis* 2014; 38: 344–353.
51. Lo EH. A new penumbra: transitioning from injury into repair after stroke. *Nat Med* 2008; 14: 497–500.
52. Ding G, Jiang Q, Li L, et al. Angiogenesis detected after embolic stroke in rat brain using magnetic resonance T2*WI. *Stroke* 2008; 39: 1563–1568.
53. Weber R, Wegener S, Ramos-Cabrer P, et al. MRI detection of macrophage activity after experimental stroke in rats: new indicators for late appearance of vascular degradation? *Magn Reson Med* 2005; 54: 59–66.
54. Brown CE, Li P, Boyd JD, et al. Extensive turnover of dendritic spines and vascular remodeling in cortical tissues recovering from stroke. *J Neurosci* 2007; 27: 4101–4109.
55. Burda JE and Sofroniew MV. Reactive gliosis and the multicellular response to CNS damage and disease. *Neuron* 2014; 81: 229–248.
56. Nakane M, Tamura A, Nagaoka T, et al. MR detection of secondary changes remote from ischemia: preliminary observations after occlusion of the middle cerebral artery in rats. *AJNR Am J Neuroradiol* 1997; 18: 945–950.

57. Zhao F, Kuroiwa T, Miyasaka N, et al. Ultrastructural and MRI study of the substantia nigra evolving exofocal post-ischemic neuronal death in the rat. *Neuropathology* 2002; 22: 91–105.
58. Justicia C, Ramos-Cabrer P and Hoehn M. MRI detection of secondary damage after stroke: chronic iron accumulation in the thalamus of the rat brain. *Stroke* 2008; 39: 1541–1547.
59. Kataoka K, Hayakawa T, Yamada K, et al. Neuronal network disturbance after focal ischemia in rats. *Stroke* 1989; 20: 1226–1235.
60. Nagasawa H and Kogure K. Exo-focal postischemic neuronal death in the rat brain. *Brain Res* 1990; 524: 196–202.
61. Prinz V, Hetzer AM, Muller S, et al. MRI heralds secondary nigral lesion after brain ischemia in mice: a secondary time window for neuroprotection. *J Cereb Blood Flow Metab* 2015; 35: 1903–1909.
62. Nudo RJ. Recovery after damage to motor cortical areas. *Curr Opin Neurobiol* 1999; 9: 740–747.
63. Ward NS. Neural plasticity and recovery of function. *Prog Brain Res* 2005; 150: 527–535.
64. Carmichael ST. Cellular and molecular mechanisms of neural repair after stroke: making waves. *Ann Neurol* 2006; 59: 735–742.
65. Murphy TH and Corbett D. Plasticity during stroke recovery: from synapse to behaviour. *Nat Rev Neurosci* 2009; 10: 861–872.
66. Dijkhuizen RM, Zaharchuk G and Otte WM. Assessment and modulation of resting-state neural networks after stroke. *Curr Opin Neurol* 2014; 27: 637–643.
67. Manoonkitiwongsa PS, Jackson-Friedman C, McMillan PJ, et al. Angiogenesis after stroke is correlated with increased numbers of macrophages: the clean-up hypothesis. *J Cereb Blood Flow Metab* 2001; 21: 1223–1231.